Synthesis and Recognition Properties of a Ruthenium(II)−Bis(zinc) Cyclic Porphyrin Trimer

Simon J. Webb*,† and Jeremy K. M. Sanders‡

Department of Chemistry, The University of Sheffield, Sheffield S3 7HF, U.K., and University Chemical Laboratory, University of Cambridge, Lensfield Road, Cambridge CB2 1EW, U.K.

Received April 12, 2000

A series of cyclic metalloporphyrin trimers containing one Ru(II)−CO porphyrin center are synthesized. A stepwise convergent route is used to synthesize **Ru(CO)Zn$_2$2·Py$_3$T**, where tripyridyltriazine (**Py$_3$T**) templates the formation of the trimer and forces the CO group to the outside of the cavity. Three mixed-metal trimers, **Ru(CO)Zn$_2$2**, **Ru(CO)Ni$_2$2**, and **Ru(CO)Mg$_2$2**, are synthesized from **Ru(CO)Zn$_2$2·Py$_3$T** and are characterized by NMR, UV−visible, and fluorescence spectroscopy. The **Ru(CO)Zn$_2$2** trimer is found to bind **Py$_3$T** very tightly ($K \approx 10^{12}$ M^{-1}), the resultant complex dissociating very slowly ($k_{dissoc} \approx 3 \times 10^{-7}$ s^{-1}) in $CDCl_3$ at 60 °C. During the course of these studies, the binding selectivity of a ruthenium porphyrin monomer, **Ru(CO)3**, for pyridine over THF is estimated to be ca. 7×10^4:1.

One of the key aims of supramolecular chemistry is to create synthetic receptors capable of recognition and catalysis. The first major milestone of our research in this area was the controlled synthesis of the trimer **Zn$_3$1** and related dimers and trimers using templated Glaser−Hay coupling of porphyrin monomers (Chart 1).[1,2] These trimers and their derivatives have proved to be useful species for intracavity recognition[1,3] and chemistry,[4] but an important part of our strategy was that we should create a series of receptors with a range of cavity sizes and recognition characteristics using diarylporphyrin monomers as the building blocks. To aid discussion and comparison of these closely related analogues, we use a shorthand notation for the number of ethyne links between building blocks. Thus the original butadiyne-linked trimer **Zn$_3$1** is denoted 2,2,2 while **Zn$_3$2** is the 1,1,2-cyclic trimer. We have previously described symmetrical trimers with larger[5] and smaller[6] cavities than **Zn$_3$1** and have also described a more versatile linear synthesis that provides access to unsymmetrical species such as **Zn$_3$2** and **NiZn$_2$2**.[4a,7] In this paper, we describe a modified version of the linear synthesis to prepare the new mixed-metal trimer **Ru(CO)Zn$_2$2** and explore some of its recognition properties, while, in the following paper,[8] we replace the zinc centers by tin(IV) to give a species with a completely new range of recognition characteristics. There have been some previous reports of mixed-metal oligoporphyrin hosts[9] but little by way of systematic study.

Our earliest efforts concentrated on zinc porphyrins because they possess a number of attractive properties: they are diamagnetic and can be readily studied spectroscopically using NMR; they can be easily prepared from free-base porphyrins but can be readily demetalated with dilute acid; and they form five-coordinate 1:1 complexes with amine ligands which have suitable binding constants for measurement by NMR spectroscopy or UV−visible titration. Expanding the repertoire of available building blocks by the addition of ruthenium centers will provide access to new properties. Ruthenium(II) carbonyl porphyrins have several useful properties for molecular recognition:

(i) They are air stable.

(ii) The ruthenium(II) center is usually six-coordinate, as expected for a d^6-configuration late transition metal.[10]

* Corresponding author. E-mail: S.J.Webb@sheffield.ac.uk.
† The University of Sheffield.
‡ University of Cambridge.

(1) (a) Sanders, J. K. M. In *Comprehensive Supramolecular Chemistry*; Atwood, J. L., Davies, J. E. D., Macnicol, D. D., Vögtle, F., Eds.; Elsevier: New York, 1996; Vol. 9, p 131. (b) Anderson, H. L.; Sanders, J. K. M. *J. Chem. Soc., Perkin Trans. 1* **1995**, 2223.
(2) (a) Anderson, S.; Anderson, H. L.; Sanders, J. K. M. *J. Chem. Soc., Perkin Trans. 1* **1995**, 2247. (b) McCallien, D. W. J.; Sanders, J. K. M. *J. Am. Chem. Soc.* **1995**, *117*, 6611.
(3) Anderson, H. L.; Anderson, S.; Sanders, J. K. M. *J. Chem. Soc., Perkin Trans. 1* **1995**, 2231.
(4) (a) Clyde-Watson, Z.; Vidal-Ferran A.; Twyman, L. J.; Walter, C. J.; McCallien, D. W. J.; Fanni, S.; Bampos, N.; Wylie, R. S.; Sanders, J. K. M. *New J. Chem.* **1998**, *22*, 493. (b) Mackay, L. G.; Wylie, R. S.; Sanders, J. K. M. *J. Am. Chem. Soc.* **1994**, *116*, 3141. (c) Marty, M.; Clyde-Watson, Z.; Twyman, L. J.; Nakash, M.; Sanders, J. K. M. *Chem. Commun.* **1998**, 2265.
(5) (a) Mackay, L. G.; Anderson, H. L.; Sanders, J. K. M. *J. Chem. Soc., Perkin Trans. 1* **1995**, 2269. (b) Anderson, H. L.; Walter, C. J.; Vidal-Ferran, A.; Hay, R. A.; Lowden, P. A.; Sanders, J. K. M. *J. Chem. Soc., Perkin Trans. 1* **1995**, 2275.
(6) Vidal-Ferran, A.; Clyde-Watson, Z.; Bampos, N.; Sanders, J. K. M. *J. Org. Chem.* **1997**, *62*, 240.
(7) Vidal-Ferran, A.; Bampos, N.; Sanders, J. K. M. *Inorg. Chem.* **1997**, *36*, 6117.
(8) Webb, S. J.; Sanders, J. K. M. *Inorg. Chem.* **2000**, *39*, 5920.
(9) (a) Cowan, J. A.; Sanders, J. K. M. *J. Chem. Soc., Perkin Trans. 1* **1987**, 2395. (b) Collman, J. P.; Arnold, H. J.; Weissman, K. J.; Burton, J. M. *J. Am. Chem. Soc.* **1994**, *116*, 9761. (c) Guilard, R.; Brandes, S.; Tardieux, C.; Tabard, A.; L'Her, M.; Miry, C.; Gouerec, P.; Knop, Y.; Collman, J. P. *J. Am. Chem. Soc.* **1995**, *117*, 11721. (d) Collin, J. P.; Gavina, P.; Heitz, V.; Sauvage, J. P. *Eur. J. Inorg. Chem.* **1998**, 1. (e) Collin, J. P.; Harriman, A.; Heitz, V.; Obobel, F.; Sauvage, J. P. *J. Am. Chem. Soc.* **1994**, *116*, 5679. (f) Harriman, A.; Sauvage, J. P. *Chem. Soc. Rev.* **1996**, *25*, 41. (g) Wagner, R. W.; Lindsey, J. S. *J. Am. Chem. Soc.* **1994**, *116*, 9759. (h) Prathapan, S.; Johnson, T. E.; Lindsey, J. S. *J. Am. Chem. Soc.* **1993**, *115*, 7519. (i) Alessio, E.; Macchi, M.; Heath, S.; Marzilli, L. G. *J. Chem. Soc., Chem. Commun.* **1996**, 1411. (j) Kariya, N.; Imamura, T.; Sasaki, Y. *Inorg. Chem.* **1998**, *37*, 1658.
(10) (a) Chow, B. C.; Cohen, I. A. *Bioinorg. Chem.* **1971**, *1*, 57. (b) Tsutsui, M.; Ostfeld, D.; Hoffman, L. M. *J. Am. Chem. Soc.* **1971**, *93*, 1820. (c) Tsutsui, M.; Ostfeld, D.; Francis, J. N.; Hoffman, L. M. *J. Coord. Chem.* **1971**, *1*, 115. (d) Bonnet, J. J.; Eaton, S. S.; Eaton, G. R.; Holm, R. H.; Ibers, J. A. *J. Am. Chem. Soc.* **1973**, *95*, 2141.

10.1021/ic000411g CCC: $19.00 © 2000 American Chemical Society
Published on Web 11/29/2000

Chart 1

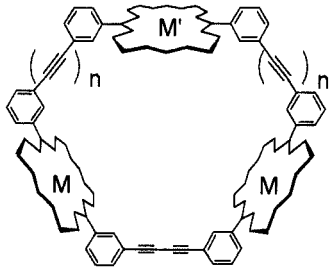

$Zn_3$1	(M = M' = Zn, n = 2)
$Zn_3$2	(M = M' = Zn, n = 1)
Ni$Zn_2$2	(M = Zn M' = Ni, n = 1)
Ru(CO)$Zn_2$2	(M = Zn M' = Ru(CO), n = 1)
Ru(CO)$Mg_2$2	(M = Mg M' = Ru(CO), n = 1)
Ru(CO)$Ni_2$2	(M = Ni M' = Ru(CO), n = 1)

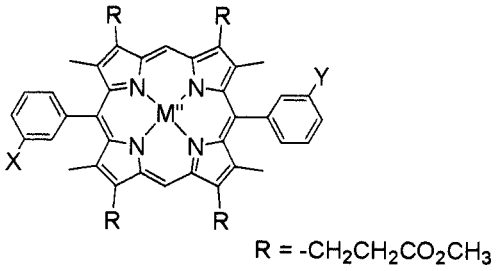

Ru(CO)3	M'' = Ru(CO), X = Y = I
Zn4	M'' = Zn, X = I, Y = C≡C-TMS
Zn5	M'' = Zn, X = C≡CH, Y = C≡C-TMS
Zn6	M'' = Zn, X = Y = C≡C-TMS

(iii) As six-coordinate d^6 ruthenium is low spin and diamagnetic, NMR spectroscopy is straightforward and ligand exchange processes at the metal are slow in comparison to those of the early transition metal porphyrins, although the sixth coordination site is somewhat labilized due to the trans effect of the carbonyl ligand. The lifetimes of amine−Ru(CO)−porphyrin complexes are sufficiently long that complexed amine and free amine are in slow exchange on the NMR chemical shift time scale;[11] this makes the spectra much easier to interpret than in the zinc case and allows direct measurement of the cooperativity of the binding of ruthenium porphyrins to bidentate ligands.[12]

(iv) Coordination of soft bases, such as sulfides, pyridines, or phosphines, is strongly favored over that of oxygen donor ligands, as expected for a low-valent late transition metal.[13] Although such coordination chemistry has been explored qualitatively, no quantitative figures are available for the strength of these binding interactions.

(v) A CO ligand effectively caps one face of a ruthenium porphyrin, forcing incoming ligands to coordinate to the opposite face. Thus, the exterior face of a cavity defined by ruthenium porphyrins can, in principle, be selectively blocked with carbonyl groups. Ligands for the ruthenium porphyrins can then only bind inside the cavity, simplifying binding and kinetic analyses. The CO group is also useful in other ways: in addition to being sensitive spectroscopically to the trans ligand, the CO group controls the chemistry of the metalloporphyrin through its electron-withdrawing effect. The carbonyl ligand can be displaced oxidatively or photolytically, or it can be displaced thermally by another π-acid, such as triphenylphosphine.[14]

(vi) In a **Ru(CO)$M_2$2** type porphyrin oligomer, the ruthenium center can be used as the reactive site within the molecule, while the substrate is bound and positioned by the other porphyrin subunits. Ruthenium porphyrins are known to catalyze a range of reactions, from the oxidation of unfunctionalized hydrocarbons to the cyclopropanoation of alkenes.[15] Provided the substrate can be bound in a specific orientation within the cavity, it can then be selectively functionalized at the position closest to the ruthenium center, leading to oxidation catalysts that mimic the selectivity of enzymes such as cytochrome P450.[16]

The ruthenium(II) carbonyl porphyrin monomer **Ru(CO)3** has been used in our laboratory in the stereospecific templated synthesis of the 2,2,2-trimer [**Ru(CO)]$_3$1** as its **Py_3T** adduct,[17] but the **Py_3T** template is so strongly held that it cannot be cleanly removed. We show here that the template can be removed from **Ru(CO)$Zn_2$2** to leave a cavity with new recognition properties. We also present what we believe to be one of the first attempts to quantitate binding processes at ruthenium porphyrin centers.

Results and Discussion

Synthesis. The route used to synthesize **Ru(CO)$Zn_2$2** was similar to that employed in the synthesis of **$Zn_3$2** and **Ni$Zn_2$2** (Schemes 1 and 2).[7] Previously, an unsymmetrical zinc monomer **Zn4** was coupled to an acetylenic symmetrical central metalloporphyrin and the ends of the resultant acyclic trimer were linked together through a Glaser coupling. However, because the conditions required for metalation of a porphyrin with ruthenium causes hydrogenation of the acetylene linkers,[18] a slightly modified strategy had to be developed. The iodo-substituted ruthenium porphyrin **Ru(CO)3** was coupled to the unsymmetrical zinc monomer **Zn5**, itself synthesized by the partial deprotection of the symmetric zinc monomer **Zn6** (Scheme 1). In the presence of **Py_3T**, this coupling afforded protected acyclic **Ru(CO)$Zn_2$2·Py_3T**, which was subsequently deprotected and cyclized (Scheme 2). The use of the **Py_3T** template was central to this synthetic strategy. The template had a 3-fold effect: (i) It facilitated the purification of both the acyclic and cyclic **Ru(CO)$Zn_2$2·Py_3T** precursors. (ii) It templated both the formation and cyclization of the trimer and inhibited the formation of higher oligomers. (iii) It directed the CO to the exterior of the cavity. Therefore, ligands for the ruthenium porphyrin were forced to bind within the cavity.

Removal of the template was only made synthetically feasible by demetalation of the zinc porphyrin subunits by acid. This

(11) Eaton, S. S.; Eaton, G. R. *Inorg. Chem.* **1977**, *16*, 72.
(12) Anderson, H. L.; Hunter, C. A.; Meah, N. M.; Sanders, J. K. M. *J. Am. Chem. Soc.* **1990**, *112*, 5780.
(13) (a) Ogoshi, H.; Sugimoto, H.; Yoshida, Z. *Bull. Chem. Soc. Jpn.* **1978**, *51*, 2369. (b) Cheng, R.-J.; Lin, S.-H.; Mo, H.-M. *Organometallics* **1997**, *16*, 2121. (c) Mashiko, T.; Dolphin, D. In *Comprehensive Coordination Chemistry*; Wilkinson, G., Ed.; Pergamon Press: New York, 1987; Chapter 21, pp 813−898.
(14) (a) Groves, J. T.; Quinn, R. *Inorg. Chem.* **1984**, *23*, 3844. (b) Hopf, F. R.; O'Brien, T. P.; Scheidt, W. R.; Whitten, D. G. *J. Am. Chem. Soc.* **1975**, *97*, 277. (c) Ariel, S.; Dolphin, D.; Domazetis, G.; James, B. R.; Leung, T. W.; Rettig, S. J.; Trotter, J.; Williams, G. M. *Can. J. Chem.* **1984**, *62*, 755.
(15) (a) Galardon, E.; Le Maux, P.; Simonneaux, G. *Chem. Commun.* **1997**, 927. (b) Ohtake, H.; Higuchi, T.; Hirobe, M. *Heterocycles* **1995**, *40*, 867. (c) Groves, J. T.; Quinn, R. *J. Am. Chem. Soc.* **1985**, *107*, 5790.
(16) Collman, J. P.; Zhang, X. M.; Lee, V. J.; Uffelman, E. S.; Brauman, J. I. *Science* **1993**, *261*, 1404.
(17) Marvaud, V.; Vidal-Ferran, A.; Webb, S. J.; Sanders, J. K. M. *J. Chem. Soc., Dalton Trans.* **1997**, 985.
(18) Anderson, H. L. Ph.D. Thesis, University of Cambridge, 1990.

Scheme 1

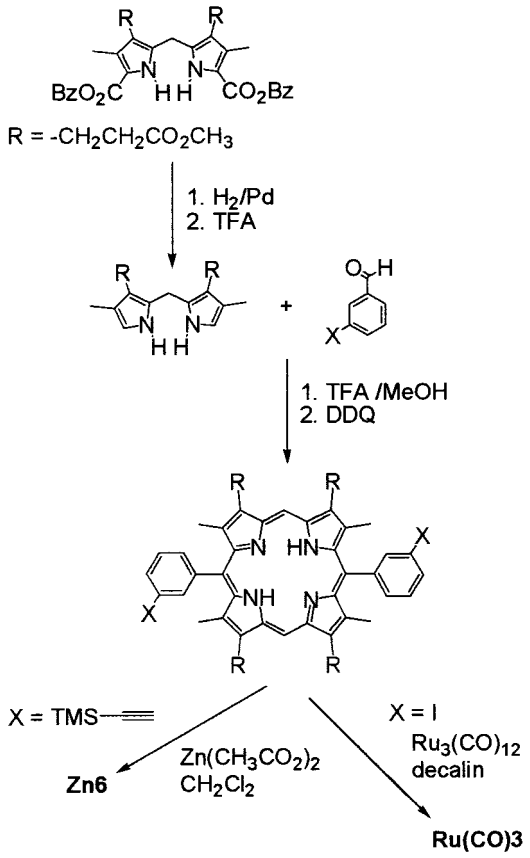

Scheme 2

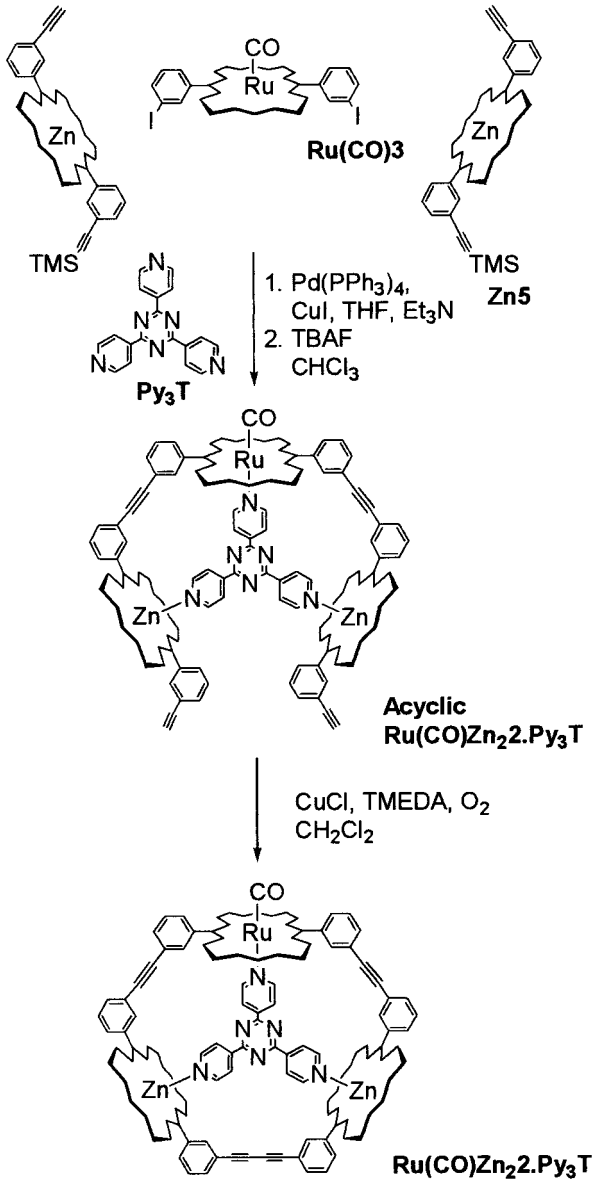

left the **Py$_3$T** bound only to the ruthenium porphyrin subunit, which was not demetalated under these conditions. The **Py$_3$T** then dissociated from the ruthenium porphyrin within a synthetically useful time scale. Washing afforded the **Ru(CO)(H$_2$)$_2$2** trimer, which could be remetalated to give heterometallic porphyrin trimers of the form **Ru(CO)M$_2$2** (Scheme 3). In this manner, several trimers were synthesized, three of which, **Ru(CO)Zn$_2$2**, **Ru(CO)Ni$_2$2**, and **Ru(CO)Mg$_2$2**, are discussed in this paper; the tin-containing **Ru(CO)M$_2$2** trimers are discussed in the following paper.[8]

Characterization. Because of the ring current of the aromatic porphyrin subunits, the proton NMR spectra of these porphyrin trimers showed very distinctive chemical shifts. The 2:1 internal stoichiometry of the trimers resulted in a 2:1 appearance of many of the resonances in the spectrum. For example, the resonances due to the meso protons, which were shifted downfield by the ring current to 9−11 ppm, integrated in a 2:1 ratio. In addition, when **Py$_3$T** was bound within the cavity of the **Ru(CO)Zn$_2$2** trimer, the resonances of the α and β protons of the template, which were strongly shielded by the aromatic ring current, were each in a 2:1 ratio. The significant resonances for the **Ru(CO)M$_2$2** compounds described in this paper are given in Table 1.

In the UV−visible spectra of both **Ru(CO)Zn$_2$2** and **Ru(CO)Ni$_2$2**, the B- and Q-bands of the component porphyrins in the trimers overlapped to give complicated spectra, with maxima at 413 and 402 nm, respectively. However, upon addition of **Py$_3$T** to **Ru(CO)Zn$_2$2**, the B-band of the zinc porphyrin subunit was red-shifted, allowing two distinct absorption bands at 404 nm [Ru(por)] and 421 nm [Zn(por)] to be observed. The UV−visible spectrum of the magnesium-containing trimer, **Ru(CO)Mg$_2$2**, displayed two clearly separated B-bands at 402 nm [Ru(por)] and 418 nm [Mg(por)], which did not change significantly upon coordination of **Py$_3$T**.

The coordination of the **Py$_3$T** ligand to **Ru(CO)Zn$_2$2** was also monitored by infrared spectroscopy. The stretching frequency of the carbonyl ligand shifted from 1936 cm^{-1} for the host to 1945 cm^{-1} for the complex. Similar changes were also observed for **Ru(CO)Mg$_2$2**.

The stabilities of the complexes were demonstrated by the detection of the parent ions for the **Py$_3$T** complexes in the FIB$^+$ mass spectra. In comparison, the **Py$_3$T** ligand was lost from the cavity of the zinc-containing **Zn$_3$2·Py$_3$T** complex under the same conditions. The strength of the ruthenium−pyridyl bond and the better fit of **Py$_3$T** within the smaller cavity of **Ru(CO)Zn$_2$2** are likely explanations for this increased stability.

The ligand **Py$_3$T** also functioned as an effective bridge for energy transfer between porphyrin subunits. The fluorescence intensity of the zinc porphyrin subunits was diminished 13-fold by the presence of the phosphorescent ruthenium porphyrin in the framework of **Ru(CO)Zn$_2$2**. Coordination of **Py$_3$T** to **Ru(CO)Zn$_2$2** resulted in a further 6-fold reduction in fluorescence intensity, implying that **Py$_3$T** acted as a bridge, improving the efficiency of energy transfer between the porphyrins.

Binding Experiments. Like **Zn$_3$2**, both **Ru(CO)Zn$_2$2** and **Ru(CO)Mg$_2$2** trimers bound **Py$_3$T** strongly, whereas **Ru(CO)-**

Scheme 3

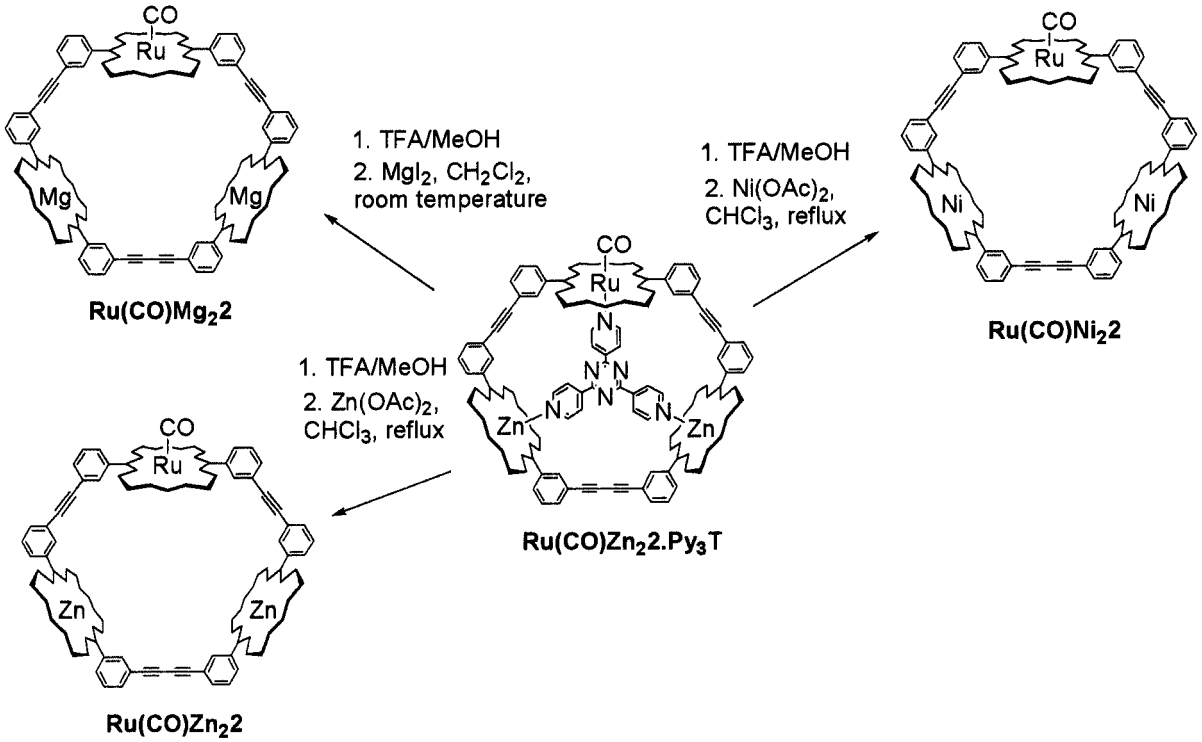

Table 1. Significant Proton NMR Resonances for **Ru(CO)M$_2$2·*n*Py$_3$T** (M = Zn, Mg, Ni; n = 0, 1)

	chemical shift (ppm)				
	Ru(CO)M$_2$2			**Ru(CO)M$_2$2·Py$_3$T**	
resonance	M = Zn	M = Mg	M = Ni	M = Zn	M = Mg
Ru(por) meso-H	9.72	9.68	9.76	9.84	9.90
M(por) meso-H	9.96	9.89	9.43	9.55	9.55
Py$_3$T α-H (Ru)				0.95	*a*
Py$_3$T α-H (M)				1.99	*a*
Py$_3$T β-H (Ru)				5.61	5.61
Py$_3$T β-H (M)				5.81	5.82

[a] Not observed due to overlapping resonances.

Ni$_2$2 did not. However, to obtain a better grasp of these binding processes, it was first necessary to understand binding to a ruthenium monomer. There is little literature published on the mechanism of coordination events at ruthenium carbonyl porphyrin centers.[11] Unlike the case of zinc porphyrins, where binding is a simple A + B process, coordination to ruthenium porphyrins may involve displacement of a ligand already coordinated to the metal center. Structure determinations have shown that ruthenium porphyrins always crystallize with a ligand, usually an alcohol, trans to the carbonyl, and it is now accepted that, in solution, there is usually a sixth ligand coordinated.[10d,19−21] Therefore, complexation of **Py$_3$T** to a ruthenium-containing trimer may involve displacement of a ligand such as water or methanol by pyridyl-containing **Py$_3$T**. The monomer **Ru(CO)3** was studied as a simple model for the study of these ligand replacement processes.

(a) Binding to a Ruthenium Monomer. The solubilities of our ruthenium carbonyl porphyrins were often dependent upon the presence or absence of a coordinating ligand in the solvent. For example, the ruthenium monomer **Ru(CO)3** was soluble in ethanol-stabilized chloroform but insoluble in dichloromethane or dry deuteriochloroform. All NMR spectra of this compound were recorded in the presence of small amounts of CD_3OD. To improve the solubility of **Ru(CO)3** in noncoordinating solvents, the methyl esters were transesterified with neopentyl alcohol to give the tetraneopentyl derivative. Though this compound was now soluble in nonpolar solvents such as hexanes in the absence of a coordinating ligand, the proton NMR spectrum recorded in dry chloroform was very complex, with broadening of all resonances of the compound. This implied that the monomer aggregated strongly, either by $\pi-\pi$ interactions or through intermolecular coordination of the ester side chains. These factors made it impossible for us to measure the affinity of a five-coordinate ruthenium carbonyl porphyrin for a sixth ligand, as our compounds were either insoluble or aggregated strongly in dry solutions.

These experiments suggested that binding of pyridyl ligands to our ruthenium porphyrin complexes was likely to be a ligand exchange process, involving displacement of coordinated water or methanol already present in solution. Thus it would be useful to know the binding selectivity of ruthenium carbonyl porphyrins for pyridine ligands over oxygen-containing ligands such as alcohols or ethers. For zinc porphyrins, this selectivity is around 500:1.[22] In a series of preliminary experiments, **Ru(CO)3** was dissolved in $CDCl_3$ that contained varying ratios of dry methanol to dry pyridine. Even at a ratio of 50:1, only ruthenium porphyrin bound to pyridine could be observed in the proton NMR spectrum (>99%). This suggested that the selectivity ratio was greater than 2500:1.

To obtain a more accurate selectivity ratio, pyridine was titrated into a THF-d_8 solution of **Ru(CO)3**, and the ratio of porphyrin with pyridine bound to porphyrin with THF-d_8 bound was monitored by proton NMR spectroscopy. Since the system

(19) Mazzanti, M.; Veyrat, M.; Ramasseul, R.; Marchon, J. C.; Turowska-Tyrk, I.; Shang, M.; Scheidt, W. R. *Inorg. Chem.* **1996**, *35*, 3733.
(20) Groves, J. T.; Han, Y. Z.; Van Engen, D. *J. Chem. Soc., Chem. Commun.* **1990**, 436.
(21) Little, R. G.; Ibers, J. A. *J. Am. Chem. Soc.* **1973**, *95*, 8583.
(22) Izatt, R. M.; Bradshaw, J. S.; Pawlak, K.; Bruening, R. L.; Tarbet, B. J. *Chem. Rev.* **1992**, *92*, 1261.

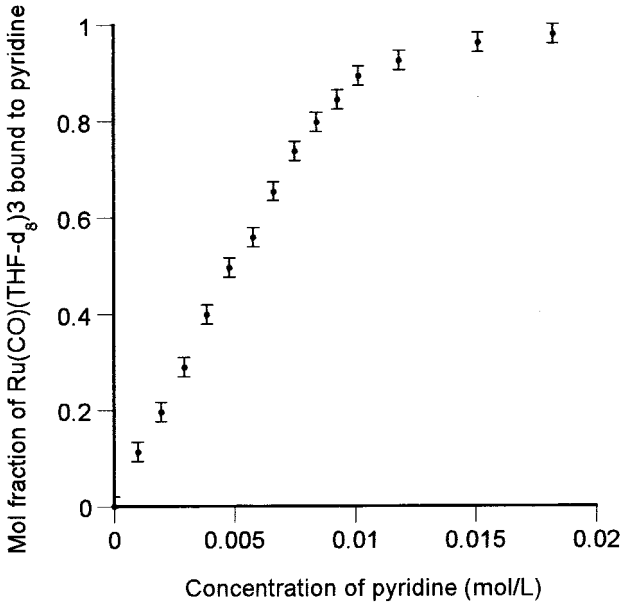

Figure 1. Graph showing the increase in **Ru(CO)(py)3** as pyridine is titrated into a 0.010 02 mol/L solution of **Ru(CO)3** in THF-d_8. The amount of **Ru(CO)(py)3** formed is expressed as the mole fraction of all ruthenium porphyrin species in solution.

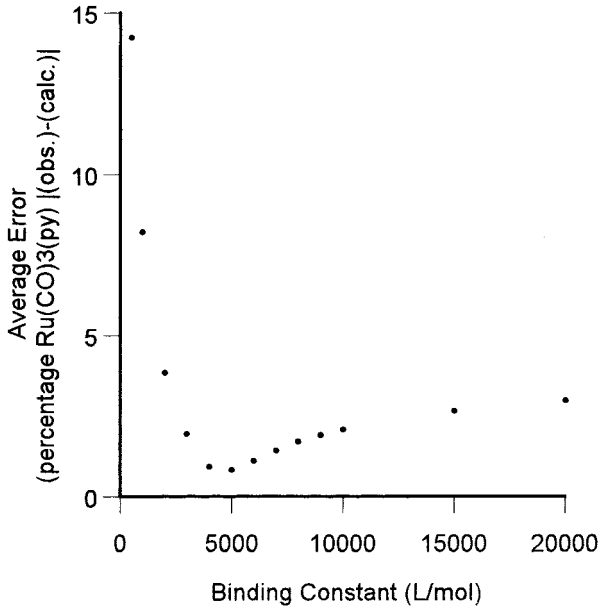

Figure 2. Plot showing variations in the average errors between values calculated at different values of the binding constant and observed experimental data for the titration of pyridine into a solution of **Ru(CO)3** in THF-d_8.

was in slow exchange, the relative proportions of each species could be directly measured by integration of the relevant resonances. Using THF-d_8 as the solvent ensured that the ruthenium porphyrin would dissolve and the concentration of the oxygen-containing ligand would remain constant at 12.3 M. Therefore, the binding process would appear to be a simple 1:1 binding event, though it was actually exchange of THF-d_8 for pyridine.

$$\mathrm{HL} + \mathrm{L}' \rightleftharpoons \mathrm{HL}' + \mathrm{L}$$

$$K = \frac{[\mathrm{HL}'][\mathrm{L}]}{[\mathrm{HL}][\mathrm{L}']} \quad \text{but since [L] = constant}$$

$$K' = \frac{[\mathrm{HL}']}{[\mathrm{HL}][\mathrm{L}']} \quad \text{and} \quad K = K'[\mathrm{L}]$$

The constant porphyrin concentration method was used for the titration.[23] The titration curve (Figure 1) shows that there is strong binding between the pyridine and the ruthenium porphyrin, as no curvature appears in the plot until nearly 0.9 equiv of pyridine had been added.[24]

By re-expressing the binding equation in terms of the percentage of ruthenium porphyrin bound as a function of pyridine added, we can simulate the binding curves for a range of relative binding constants.

$$[\mathrm{HL}'] = \left\{\left([\mathrm{HL}]_0 + [\mathrm{L}']_0 + \frac{1}{K'}\right) \pm \left[\left(-[\mathrm{HL}]_0 - [\mathrm{L}']_0 - \frac{1}{K'}\right)^2 - 4[\mathrm{HL}]_0[\mathrm{L}']_0\right]^{1/2}\right\}/2$$

Figure 2 shows that as the simulated binding constant is increased from 500 to 20 000 M^{-1}, the best fit to the experimental data is at $K' \approx 5000$ M^{-1}. The estimated error in the measurements is ±0.02, which gives a range for the binding constant K between 3000 and 9500 M^{-1}. By factoring in the molarity of the solvent, THF-d_8, we calculate the selectivity for pyridine over THF to be $(7 \pm 3) \times 10^4$:1.

(b) Binding to Ru(CO)Zn$_2$2. The **Ru(CO)Zn$_2$2**−**Py$_3$T** binding constant could not be measured directly using UV−visible spectroscopic titration because the largest binding constants that can be measured by this method are on the order of 10^{10} M^{-1}.[25] The **Py$_3$T**−**Ru(CO)Zn$_2$2** binding constant was expected to be equal to or greater than the **Py$_3$T**−**Zn$_3$2** binding constant, which has a value of 5×10^9 M^{-1} in CH_2Cl_2.[7] A more accurate method is to use an ^{1}H NMR competition experiment between two different hosts, for one of which the **Py$_3$T**-binding constant is known. The **Py$_3$T** will be bound within one host, and the rate at which it transfers to the other host will give the off-rate of the ligand leaving the original complex. The equilibrium position between the two hosts provides the unknown binding constant for the new host.

Experimental evidence had indicated that binding of **Py$_3$T** to **Ru(CO)Zn$_2$2** was likely to be far greater than binding to the all-zinc analogue **Zn$_3$2**; hence the stronger binding hexanitro trimer **Zn$_3$1(NO$_2$)$_6$** was chosen as the competing host.[25] Initially the **Py$_3$T**−**Ru(CO)Zn$_2$2** binding constant was to be determined by finding the equilibrium ratio between **Ru(CO)Zn$_2$2·Py$_3$T** and **Zn$_3$1(NO$_2$)$_6$** (reaction A, Scheme 4). However, attempts to determine the binding constant and off-rate at 22 °C were abandoned, as no reaction was observed after 1 week. We suspected that the lack of reaction was due to the slow off-rate of **Py$_3$T** leaving **Ru(CO)Zn$_2$2·Py$_3$T** at this temperature, as might be anticipated for a ruthenium porphyrin containing system. Thus the sample was heated to 60 °C, and at this temperature, some reaction was observed after a period of a few days. However, even at this elevated temperature, the reaction was very slow, and after several months, the reaction still did not appear to be approaching equilibrium. Although these measurements provided the off-rate of the **Py$_3$T** ligand leaving **Ru(CO)Zn$_2$2·Py$_3$T**, the slow reaction rate gave no guarantee that equilibration could be achieved within a reason-

(23) Levy, E. G. Ph.D. Thesis, University of Cambridge, 1996.

(24) Since K' is obviously very high, the assumption that $[L_0] - [L] \sim [L_0]$ is not valid, ruling out Lineweaver−Burke and Hill plots as useful analytical methods.

(25) McCallien, D. J. M. Ph.D. Thesis, University of Cambridge, 1995.

Scheme 4

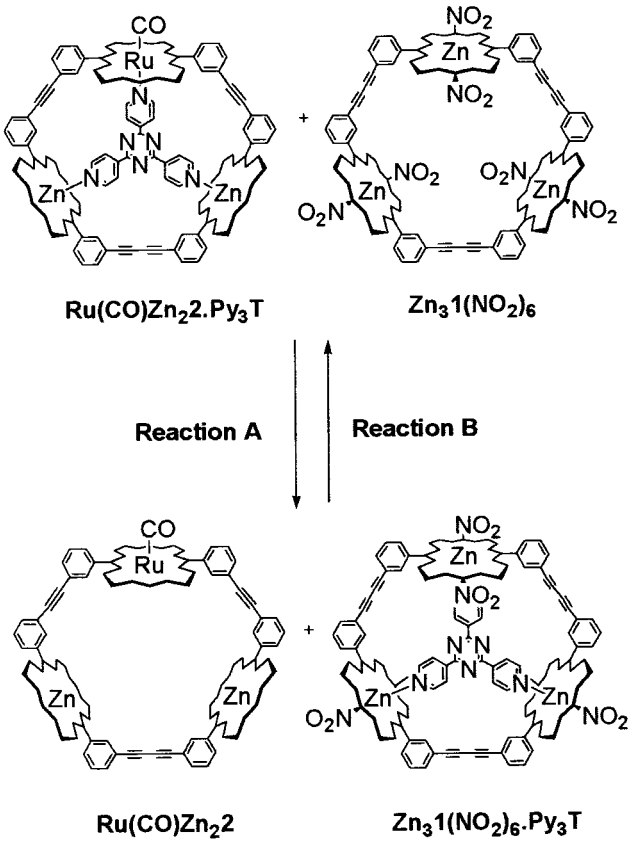

able time period. To find the equilibrium position, the reverse reaction, transfer of **Py$_3$T** from **Zn$_3$1(NO$_2$)$_6$·Py$_3$T** to **Ru(CO)Zn$_2$2**, was also monitored at 60 °C (reaction B, Scheme 4). In this case, the experiment nearly reached equilibrium after 9 min and had equilibrated after 2 h at 60 °C.

The [**Ru(CO)Zn$_2$2·Py$_3$T**]:[**Zn$_3$1(NO$_2$)$_6$·Py$_3$T**] equilibrium ratio at 60 °C in $CDCl_3$ was found to be (52 ± 1):(48 ± 1). The estimated constant for **Zn$_3$1(NO$_2$)$_6$** binding to **Py$_3$T** in $CDCl_3$ at 60 °C is 1×10^{12} M^{-1}, so the estimated constant for **Ru(CO)Zn$_2$2** binding to **Py$_3$T** at this temperature is also around 1×10^{12} M^{-1}.[25] This is significantly higher than the value of 5×10^9 M^{-1} measured at 30 °C for **Zn$_3$2**, which has the same cavity size. This confirms the much higher affinity of pyridine donor ligands for ruthenium porphyrins than for zinc porphyrins.

The off-rate was determined from the initial rate of **Py$_3$T** transfer from **Ru(CO)Zn$_2$2·Py$_3$T** to **Zn$_3$1(NO$_2$)$_6$**. The initial rate of **Py$_3$T** loss at $t = 0$ yields a value for the rate constant of $(3 \pm 1) \times 10^{-7}$ s^{-1}. This off-rate constant is significantly lower than those observed for **Zn$_3$1·Py$_3$T** (220 s^{-1} at 93 °C) and **Zn$_3$1(NO$_2$)$_6$·Py$_3$T** (9.3×10^{-5} s^{-1} at 60 °C), but this was not unexpected as the exchange rates of pyridines bound to ruthenium porphyrins are known to be slow.[11,25]

The on-rate constants for both hosts can be calculated using the expression $k_{on} = K(k_{off})$. Thus, k_{on} for **Ru(CO)Zn$_2$2** (3×10^5 mol^{-1} s^{-1} L in $CDCl_3$ at 60 °C) is approximately 300 times lower than that for **Zn$_3$1(NO$_2$)$_6$** (9×10^7 mol^{-1} s^{-1} L in $CDCl_3$ at 60 °C). The displacement by the incoming **Py$_3$T** of an existing ligand, such as water, already coordinated to the ruthenium center is a likely explanation for this difference, especially since our previous experiments with ruthenium monomers suggest five-coordinate ruthenium porphyrins have high affinities for sixth ligands. Water is the most likely candidate for an adventitious ligand, since all NMR spectra showed a significant concentration of dissolved water. If we consider that binding to a ruthenium porphyrin is known to proceed via a dissociative mechanism,[11] then the true on-rate (k_{on}(actual)) is the rate of **Py$_3$T** reacting with this host containing five-coordinate ruthenium.

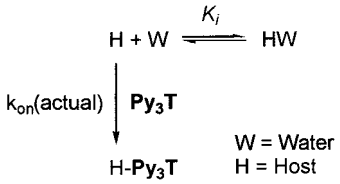

Therefore

$$k_{on}(\text{measd}) = \frac{k_{on}(\text{actual})}{1 + K_i[\text{W}]}$$

Generally, for zinc porphyrins, the product K_i[W] is not a significant factor. However, our experiments suggest that, for ruthenium carbonyl porphyrins, K_i may be much higher than those for zinc porphyrins and thus may have an effect on k_{on}(measd) even at low concentrations of water. However, other possible reasons for the slow on-rate cannot be excluded, such as a conformational change at the ruthenium porphyrin upon coordination of **Py$_3$T**.

Conclusions

A stepwise synthetic strategy can be used to prepare unsymmetrical ruthenium-containing porphyrin trimers. Incorporating ruthenium carbonyl porphyrins provides access to a new set of recognition properties complementary to those of zinc porphyrins. Ruthenium porphyrins are shown to have slower exchange rates and higher selectivities for pyridyl-containing ligands compared to zinc porphyrins. This is manifested in the very high affinity of **Py$_3$T** for **Ru(CO)Zn$_2$2** and the very slow dissociation rate for the resultant complex **Ru(CO)Zn$_2$2·Py$_3$T**.[26] Furthermore, the zinc ions in **Ru(CO)Zn$_2$2** can be replaced with other metals such as nickel and magnesium to give trimers containing porphyrins with divergent recognition properties.

These ruthenium-containing trimers allow access to the rich redox and catalytic chemistry of ruthenium porphyrins and open a pathway to possible shape-selective catalysts.

Experimental Section

General Information. NMR spectra were obtained on Bruker AC 250, DPX 250, AM 400, WM 400, and DRX 500 spectrometers, infrared spectra on a Perkin-Elmer 1710 spectrometer, and UV−visible spectra on a Uvikon 810 spectrophotometer. FAB^+/FIB^+ mass spectra were recorded on a Kratos MS-50 spectrometer using a *m*-nitrobenzyl alcohol matrix, and MALDI-TOF mass spectra were acquired on a Kratos Kompact MALDI-2 spectrometer. Fluorescence spectra were recorded on a Shimadzu RF-5001PC spectrofluorometer in the emission mode with excitation at 411 nm. Porphyrin trimer samples were 1 μM in dry argon saturated dichloromethane, and zinc monomer samples were 2 μM in dry argon saturated dichloromethane.

(26) This powerful binding has been exploited to create multiporphyrin arrays of various geometries: (a) Darling, S. L.; Mak, C.-C.; Bampos, N.; Feeder, N.; Teat, S. J.; Sanders, J. K. M. *New J. Chem.* **1999**, *23*, 359. (b) Mak, C.-C.; Bampos, N.; Sanders, J. K. M. *Chem. Commun.* **1999**, 1085. (c) Kim, H.-J.; Bampos, N.; Sanders, J. K. M. *J. Am. Chem. Soc.* **1999**, *121*, 8120. (d) Prodi, A.; Indelli, M. T.; Kleverlaan, C. J.; Scandola, F.; Alessio, E.; Gianferrara, T.; Marzilli, L. G. *Chem. Eur. J.* **1999**, *5*, 2668. (e) Darling, S. L.; Stulz, E.; Feeder, N.; Bampos, N.; Sanders, J. K. M. *New J. Chem.* **2000**, *24*, 261.

Column chromatography was carried out on 60 mesh silica gel or alumina UG1 unless otherwise stated. All solvents were distilled before use. **Zn5**,[3] **Py$_3$T**,[3] **Ru(CO)3**,[17] and CuCl[27] were all prepared according to known procedures. Recrystallization was performed either by layering methanol onto a concentrated solution of the porphyrin in chloroform or by adding hexanes or methanol to a dichloromethane or chloroform solution of the porphyrin, followed by slow removal of the solvent on a rotary evaporator.

The resonances due to carbonyls bound to ruthenium porphyrins are too weak to be observed in the ^{13}C NMR spectra and can only be observed if the samples are isotopically enriched with ^{13}CO.[28]

Preparation of Deprotected Acyclic Ru(CO)Zn$_2$2·Py$_3$T. Pd(PPh$_3$)$_4$ (44 mg, 0.038 mmol), CuI (14.5 mg, 0.076 mmol), **Py$_3$T** (120 mg, 0.38 mmol), the monoprotected zinc monomer **Zn5** (400 mg, 0.396 mmol), and the ruthenium monomer **Ru(CO)3** (200 mg, 0.157 mmol) were placed in a 500 mL three-necked round-bottomed flask; the flask was then evacuated and filled with argon. To this mixture was added THF (125 mL), followed by Et$_3$N (125 mL). The red-orange solution was degassed three times and then freeze−thaw−pump-degassed once. The resulting solution was heated to reflux for 3 h, until TLC indicated complete reaction (silica gel/1:1:2 ethyl acetate/hexanes/chloroform). After cooling, the solvent was removed under reduced pressure. The residue was purified by column chromatography (silica gel/1:1:2 ethyl acetate/hexanes/chloroform), removing the catalyst and excess porphyrin monomer. The purple-red product band was collected, and the solvent was removed under reduced pressure to provide crude protected acyclic **Ru(CO)Zn$_2$2·Py$_3$T** (527 mg).

The crude product obtained above was dissolved in chloroform (170 mL), and TBAF (1 M solution in THF, 1.25 mL, 1.25 mmol) was added. The mixture was degassed three times, heated to reflux for 20 min, allowed to cool to room temperature under argon, and then stirred for 0.5 h. CaCl$_2$ was added (excess), and the resulting mixture was washed with distilled water (3 × 140 mL) and dried (MgSO$_4$). After filtration, the solvent was removed from the solid under reduced pressure and the residue was purified by column chromatography (silica gel/1:1:2 ethyl acetate/hexanes/dichloromethane). After collection of the purple-red product band, the solvent was changed to 1% methanol in chloroform. The band that eluted with this solvent system was collected, and the solvent was removed under reduced pressure. More **Ru(CO)-Zn$_2$2·Py$_3$T** product was obtained from this band by repeating the column chromatography as described previously. After repetition of this procedure twice, the residue largely consisted of the linear tetramer. The solvent was removed from the combined product bands, to give pure deprotected acyclic **Ru(CO)Zn$_2$2·Py$_3$T** (234 mg, 46% yield from the ruthenium monomer **Ru(CO)3**). The residue was 1:1.1 trimer/tetramer, 142 mg. Anal. Calcd for $C_{183}H_{164}N_{18}O_{25}Zn_2Ru$: C, 67.7; H, 5.1; N, 7.8. Found: C, 67.4; H, 5.1; N, 7.6. IR ($CHCl_3$; cm^{-1}): ν_{CO} = 1947. ^{1}H NMR ($CDCl_3$): δ 0.95 (d, 6.6 Hz, 2H, α-H of **Py$_3$T**-Ru); 1.98 (m, 4H, α-H of **Py$_3$T**-Zn); 2.40 (s), 2.41 (s), 2.43 (s), 2.47 (s) (36H, −CH$_3$,); 2.95 (m, 26H, −CH$_2$C*H*$_2$CO$_2$CH$_3$, −CC−H); 3.42 (s), 3.43 (s), 3.44 (s), 3.47 (s), 3.48 (s) (36H, −CH$_2$CH$_2$CO$_2$C*H*$_3$); 3.99 (m, 8H, C*H*$_2$CH$_2$CO$_2$CH$_3$ of Ru(Por) subunit); 4.11 (m, 16H, C*H*$_2$CH$_2$-CO$_2$CH$_3$ of Zn(Por) subunits); 5.58 (d, 6.6 Hz, 2H, β-H of **Py$_3$T**-Ru); 5.78 (m, 4H, β-H of **Py$_3$T**-Zn); 7.41−8.39 (m, 24H, aromatic); 9.53 (s, 2H, meso-H of Ru(Por) subunit); 9.83 (s, 4H, meso-H of Zn(Por) subunits).^{13}C NMR ($CDCl_3$): δ 15.60, 15.69, 21.74, 21.90, 36.70, 37.01, 51.54, 90.30, 90.44, 96.88, 98.76, 117.90, 118.52, 118.93, 119.90, 122.37, 122.51, 128.03, 132.19, 132.98, 133.46, 135.35, 135.78, 136.27, 136.99, 138.16, 138.37, 140.02, 140.49, 140.72, 141.21, 141.28, 143.39, 143.56, 144.21, 144.43, 144.99, 145.78, 147.37, 147.44, 167.79, 168.38, 173.55. λ_{max} ($CHCl_3$)/nm: 404, 420, 520 (sh), 551, 584. Mass spectral data (*m*/*z*): calculated for $C_{183}H_{164}N_{18}O_{25}Zn_2Ru$ (average molecular weight for cluster) 3247.30; MALDI-TOF found 2909.23 ([M − **Py$_3$T** − CO + 2H]$^+$); FIB$^+$ found 2936 ([M − **Py$_3$T** + H]$^+$).

Preparation of Ru(CO)Zn$_2$2·Py$_3$T. Deprotected acyclic **Ru(CO)-Zn$_2$2·Py$_3$T** (234 mg, 0.072 mmol) and freshly prepared CuCl (521 mg, 5.26 mmol) were added to a 1 L round-bottomed flask, followed by dry dichloromethane (306 mL) and TMEDA (474 μL, 5.28 mmol). The mixture was stirred under dry air for 24 h and then washed with distilled water (3 × 220 mL), after which the organic phase was dried (MgSO$_4$) and filtered and the solvent was removed under reduced pressure. The residue was then purified by column chromatography (silica gel/1:1:2 ethyl acetate/hexanes/chloroform). The band that eluted was collected, and the solvent was removed under reduced pressure. The red-purple residue was recrystallized from dichloromethane/hexanes, filtered off, and washed with ethanol followed by hexanes to afford pure **Ru(CO)Zn$_2$2·Py$_3$T** (123 mg, 53% yield). Anal. Calcd for $C_{183}H_{162}N_{18}O_{25}Zn_2Ru\cdot 2H_2O$: C, 67.0; H, 5.1; N, 7.7. Found: C, 67.0; H, 5.0; N, 7.6. IR ($CHCl_3$; cm^{-1}): ν_{CO} = 1945 (br). ^{1}H NMR ($CDCl_3$): δ 0.95 (split d, 5.3 Hz, 2H, α-H of **Py$_3$T**-Ru); 1.99 (split d, 1.5 Hz, 5.05 Hz, 4H, α-H of **Py$_3$T**-Zn); 2.42 (s), 2.46 (s), 2.51 (s) (36H, −CH$_3$); 2.98 (m, 24H, −CH$_2$C*H*$_2$CO$_2$CH$_3$); 3.43 (s), 3.45 (s), 3.48 (s) (36H, −CH$_2$CH$_2$CO$_2$C*H*$_3$); 4.01 (m, 8H, C*H*$_2$CH$_2$CO$_2$CH$_3$ of Ru(Por) subunit), 4.12 (m, 16H, C*H*$_2$CH$_2$CO$_2$CH$_3$ of Zn(Por) subunits); 5.61 (split d, 1.5 Hz, 5.2 Hz, 2H, β-H of **Py$_3$T**-Ru); 5.81 (split d, 1.6 Hz, 4.9 Hz, 4H, β-H of **Py$_3$T**-Zn); 7.67−8.50 (m, 24H, aromatic); 9.55 (s, 2H, meso-H of Ru(Por) subunit); 9.84 (s, 4H, meso-H of Zn(Por) subunits).^{13}C NMR ($CDCl_3$): δ 15.52, 15.60, 15.69, 21.73, 21.87, 36.69, 36.97, 51.49, 51.53, 90.29, 90.42, 96.80, 98.73, 117.40, 117.98, 118.51, 120.00, 120.72, 122.34, 122.46, 128.06, 130.99, 131.98, 133.36, 135.57, 136.00, 137.90, 138.11, 138.39, 140.16, 140.47, 140.65, 141.22, 141.26, 143.35, 143.57, 144.44, 145.07, 145.69, 145.77, 147.18, 147.45, 168.52, 173.50, 173.56. λ_{max} ($CHCl_3$)/nm: 404, 421, 520 (sh), 551, 584. Mass spectral data (*m*/*z*): calculated for $C_{183}H_{162}N_{18}O_{25}Zn_2Ru$ (average molecular weight for cluster) 3245.28; MALDI-TOF found 2903.63 ([M − **Py$_3$T** − CO]$^+$); FIB$^+$ found 3245, 2935 ([M]$^+$, [M − **Py$_3$T** + 2H]$^+$).

Preparation of Ru(CO)Zn$_2$2. Ru(CO)Zn$_2$2·Py$_3$T (50 mg, 0.015 mmol) was dissolved in chloroform (75 mL), 20% methanol in TFA (25 mL) was added, and the resulting green solution was stirred for 10 min. The mixture was washed with distilled water (4 × 75 mL), and the organic layer was then dried (MgSO$_4$) and filtered. Zinc(II) acetate (50 mg, 0.27 mmol) was added to the filtrate, and the mixture was heated to reflux for 5 min, after which it was allowed to stir at room temperature for 0.5 h. The resulting purple solution was filtered through Celite, and the solvent was removed from the filtrate under reduced pressure. The residue was dissolved in chloroform (75 mL), the resulting solution was treated with 20% methanol in TFA (25 mL), and the above procedure was repeated. The purple-red residue obtained was purified by column chromatography (silica gel/1% methanol in chloroform). One main red band was obtained; this was collected, and the solvent was removed under reduced pressure. The residue obtained was recrystallized from 1% methanol in dichloromethane/hexanes, filtered off, and washed with hexanes (37 mg, 82% yield). Anal. Calcd for $C_{166}H_{154}N_{12}O_{26}Zn_2Ru\cdot 3H_2O$: C, 66.4; H, 5.3; N, 5.6. Found: C, 66.5; H, 5.1; N, 5.5. IR (1% methanol in $CHCl_3$; cm^{-1}): ν_{CO} = 1936 (br). ^{1}H NMR ($CDCl_3$/CD_3OD): δ 2.34 (s), 2.35 (s), 2.43 (s) (36H, −CH$_3$); 3.00 (br t, 24H, −CH$_2$C*H*$_2$CO$_2$CH$_3$); 3.50 (s), 3.55 (s), 3.56 (s) (36H, −CH$_2$CH$_2$CO$_2$C*H*$_3$); 4.09 (br t, 8H, C*H*$_2$CH$_2$CO$_2$CH$_3$ of Ru(Por) subunit); 4.11 (br t, 16H, C*H*$_2$CH$_2$CO$_2$CH$_3$ of Zn(Por) subunits); 7.68−8.11 (m, 24H, aromatic); 9.72 (s, 2H, meso-H of Ru(Por) subunit); 9.96 (s, 4H, meso-H of Zn(Por) subunits). ^{13}C NMR ($CDCl_3$): δ 15.51, 15.61, 36.81, 37.01, 51.67, 90.03, 90.11, 96.78, 98.58, 117.66, 118.28, 119.00, 119.09, 121.01, 122.27, 122.51, 127.72, 131.68, 133.10, 133.72, 135.60, 135.77, 137.25, 138.17, 138.28, 138.34, 138.57, 140.69, 140.95, 141.16, 143.23, 144.07, 144.21, 145.75, 145.80, 147.21, 147.36, 173.86, 173.96. λ_{max} ($CHCl_3$)/nm: 413, 543, 575. Mass spectral data (*m*/*z*): calculated for $C_{166}H_{154}N_{12}O_{26}Zn_2Ru$ (average molecular weight for cluster) 2964.97; MALDI-TOF found 2903.93 ([M − CH_3OH − CO − H]$^+$).

Preparation of Ru(CO)Ni$_2$2. Ru(CO)Zn$_2$2·Py$_3$T (30 mg, 9 μmol) was dissolved in chloroform (45 mL), 20% methanol in TFA (45 mL) was added, and the resulting green solution was stirred for 10 min. The mixture was washed with distilled water (4 × 45 mL), the organic layer was dried (MgSO$_4$) and filtered, and the solvent was removed under reduced pressure. The purple-red residue was redissolved in 1% methanol in chloroform (9 mL), and nickel acetate tetrahydrate (23.4 mg, 94 μmol, 10 equiv) was added. The mixture was degassed three times at room temperature and then heated to reflux for 24 h. After

(27) Keller, R. N.; Wycoff, H. D. *Inorg. Synth.* **1946**, *2*, 1.
(28) Eaton, S. S.; Eaton, G. R. *Inorg. Chem.* **1976**, *15*, 134.

cooling, the purple solution was filtered through Celite, and the solvent was removed from the filtrate under reduced pressure. The purple-red residue obtained was purified by column chromatography (silica gel/1% methanol in chloroform). The solvent was removed from the product, and the residue was dissolved in chloroform (45 mL), and the resulting solution was treated with 20% methanol in TFA (15 mL) to remove bound **Py_3T**. The mixture was washed with distilled water (4 × 45 mL), and the organic layer was then dried ($MgSO_4$) and filtered. The solvent was removed from the filtrate under reduced pressure to give a red solid. The residue obtained was recrystallized from 1% methanol in dichloromethane/hexanes (15 mg, 55% yield). Anal. Calcd for $C_{166}H_{154}N_{12}O_{26}Ni_2Ru{\cdot}CH_3OH{\cdot}3CH_2Cl_2$: C, 63.3; H, 5.0; N, 5.2. Found: C, 63.4; H, 5.0; N, 5.3. IR ($CHCl_3$; cm^{-1}): ν_{CO} = 1932. ^1H NMR ($CDCl_3/CD_3OD$): δ 2.13 (s), 2.24 (s), 2.35 (s) (36H, $-CH_3$); 2.85 (br t, 16H, $-CH_2CH_2CO_2CH_3$ of Ni(Por) subunits); 3.02 (br t, 8H, $-CH_2CH_2CO_2CH_3$ of Ru(Por) subunit); 3.53 (s), 3.61 (s), 3.62 (s) (36H, $-CH_2CH_2CO_2CH_3$); 3.92 (br t, 16H, $CH_2CH_2CO_2CH_3$ of Ni(Por) subunits); 4.11 (br t, 8H, $CH_2CH_2CO_2CH_3$ of Ru(Por) subunit); 7.27−8.22 (m, 24H, aromatic); 9.43 (s, 4H, meso-H of Ni(Por) subunits); 9.76 (s, 2H, meso-H of Ru(Por) subunit). ^{13}C NMR ($CDCl_3$): δ 15.40, 15.66, 21.37, 21.84, 29.73, 36.40, 36.82, 51.64, 51.72, 74.24, 81.61, 89.66, 89.80, 90.16, 90.29, 96.22, 98.68, 115.77, 116.38, 119.00, 121.17, 122.13, 122.45, 122.77, 127.02, 127.87, 128.30, 129.10, 131.77, 132.14, 132.72, 133.21, 133.54, 134.37, 134.91, 135.70, 138.22, 139.32, 139.60, 140.57, 140.78, 141.25, 141.41, 141.67, 141.95, 143.18, 173.36, 173.79. λ_{max} ($CHCl_3$)/nm: 402, 526, 561. Mass spectral data (*m*/*z*): calculated for $C_{166}H_{154}N_{12}O_{26}Ni_2Ru$ (average molecular weight for cluster) 2919.57; MALDI-TOF found 2925.30 ($[M + 5H]^+$).

Preparation of Ru(CO)$Mg_2$2. Ru(CO)$Zn_2$2·Py_3T (10 mg, 3 μmol) was dissolved in chloroform (25 mL), 20% methanol in TFA (5 mL) was added, and the resulting green solution was stirred for 10 min. The mixture was washed with distilled water (4 × 75 mL), the organic layer was dried ($MgSO_4$) and filtered, and the solvent was removed from the filtrate under reduced pressure. The red residue was dissolved in chloroform (25 mL), and 20% methanol in TFA (5 mL) was added. The green solution that resulted was stirred for 10 min. The mixture was then washed with distilled water (4 × 75 mL), and the organic layer was dried ($MgSO_4$). The red solution was filtered, and the solvent was removed from the filtrate under reduced pressure. The residue was redissolved in dry dichloromethane (1 mL); then dry triethylamine (33 μL, 0.24 mmol) and anhydrous MgI_2 (33 mg, 0.12 mmol) were added. The slurry was stirred for 45 min, after which the reaction mixture was purified by column chromatography (1% triethylamine in chloroform/alumina). The single band obtained was fractionated, and the fractions were analyzed by UV−visible spectroscopy. The product-containing fractions were combined, and the solvent was removed under reduced pressure, affording **Ru(CO)$Mg_2$2** as a red solid (6.2 mg, 70% yield). Anal. Calcd for $C_{166}H_{154}N_{12}O_{26}Mg_2Ru{\cdot}3CH_3OH{\cdot}2CH_2Cl_2$: C, 65.5; H, 5.4; N, 5.4. Found: C, 65.4; H, 5.4; N, 5.5. IR (1% methanol in $CHCl_3$; cm^{-1}): ν_{CO} = 1935 (br). ^1H NMR ($CDCl_3/CD_3OD$): δ 2.30 (s), 2.39 (s) (36H, $-CH_3$); 2.97 (br m, 24H, $-CH_2CH_2CO_2CH_3$); 3.47 (s), 3.51 (s), 3.52 (s) (36H, $-CH_2CH_2CO_2CH_3$); 4.03 (br t, 8H, $CH_2CH_2CO_2CH_3$ of Ru(Por) subunit); 4.16 (br t, 16H, $CH_2CH_2CO_2CH_3$ of Mg(Por) subunits); 7.62−8.10 (m, 24H, aromatic); 9.68 (s, 2H, meso-H of Ru(Por) subunit); 9.89 (s, 4H, meso-H of Mg(Por) subunits). ^{13}C NMR ($CDCl_3$): δ 15.38, 15.60, 21.94, 36.73, 37.07, 51.59, 89.92, 90.06, 90.12, 90.24, 97.46, 98.49, 118.31, 118.35, 118.91, 118.96, 120.80, 122.20, 122.28, 127.37, 127.55, 127.63, 127.83, 129.01, 131.41, 131.50, 131.70, 132.49, 132.97, 133.61, 135.48, 135.73, 137.19, 138.10, 138.15, 138.22, 138.45, 140.59, 140.86, 141.06, 143.10, 144.50, 144.64, 145.46, 145.52, 146.82, 146.98, 173.85, 173.88. λ_{max} ($CHCl_3$)/nm: 402, 418, 523, 553, 587. Mass spectral data (*m*/*z*): calculated for $C_{166}H_{154}N_{12}O_{26}Mg_2Ru$ (average molecular weight for cluster) 2882.82; FIB^+ found 2851.5 ($[M - CH_3OH + H]^+$).

Preparation of Ru(CO)$Mg_2$2·Py_3T. Ru(CO)$Mg_2$2 (6.2 mg, 2.2 μmol) was dissolved in $CDCl_3$ (1 mL), and tripyridyltriazine (1.0 mg, 3.2 μmol) was added. After removal of the solvent under reduced pressure, the residue was purified by column chromatography (silica gel/1:1:2 ethyl acetate/hexanes/chloroform with 1% triethylamine). The single band collected was fractionated, and the fractions were analyzed by UV−visible spectroscopy. The product-containing fractions were combined, and the solvent was removed under reduced pressure to give a red-purple residue (4.0 mg, 58% yield). IR (1% methanol in $CHCl_3$; cm^{-1}): ν_{CO} = 1946 (br). ^1H NMR ($CDCl_3/CD_3OD$): δ 2.43 (s), 2.46 (s), 2.52 (s) (36H, $-CH_3$); 2.95 (br m, 24H, $-CH_2CH_2CO_2CH_3$); 3.43 (s), 3.45 (s), 3.49 (s) (36H, $-CH_2CH_2CO_2CH_3$); 4.00 (br t, 8H, $CH_2CH_2CO_2CH_3$ of Ru(Por) subunit); 4.15 (br t, 16H, $CH_2CH_2CO_2CH_3$ of Mg(Por) subunits); 5.61 (split d, 1.5 Hz, 6.8 Hz, 2H, β-H of **Py_3T**-Ru); 5.82 (split d, 1.6 Hz, 4.9 Hz, 4H, β-H of **Py_3T**-Mg); 7.74−8.51 (m, 24H, aromatic); 9.55 (s, 2H, meso-H of Ru(Por) subunit); 9.90 (s, 4H, meso-H of Mg(Por) subunits). λ_{max} ($CHCl_3$)/nm: 402, 418, 523, 553, 587. Mass spectral data (*m*/*z*): calculated for $C_{183}H_{164}N_{18}O_{25}Mg_2Ru$ (average molecular weight for cluster) 3163.1; FIB^+ found 3164.2 ($[M + H]^+$).

Binding of Pyridine to Ru(CO)3. Ru(CO)3 (19.14 mg, 1.500 μmol) was dissolved in THF-d_8 (1.500 μL) to give a 0.010 02 mol/L standard solution, of which 0.900 mL was added to an NMR tube (9.015 μmol of **Ru(CO)3**). Pyridine (dried over KOH and filtered before use; 5.67 mg, 74.2 μmol) was dissolved in THF-d_8 (0.500 mL) to provide a 0.148 mol/L standard solution. Aliquots of this standard solution (6 μL) were added to the **Ru(CO)3** solution, and a 250 MHz ^1HNMR spectrum was recorded after each addition. The ratio of **Ru(CO)(THF-d_8)3** to **Ru(CO)(py)3** was determined by integration of the respective ruthenium meso-H resonances.

Competition Experiment between Ru(CO)$Zn_2$2·Py_3T and $Zn_3$1$(NO_2)_6$. Ru(CO)$Zn_2$2·Py_3T (3.020 mg, 0.9306 μmol) was dissolved in $CDCl_3$ (0.850 mL); then **$Zn_3$1$(NO_2)_6$** was added (2.805 mg, 0.8801 μmol), and the mixture was incubated at 60 °C for 2 months. The extent of **Py_3T** transfer was calculated from the integrals of the bound **Py_3T** resonances in the 250 MHz ^1H NMR spectrum.

Competition Experiment between $Zn_3$1$(NO_2)_6$·Py_3T and Ru(CO)$Zn_2$2. $Zn_3$1$(NO_2)_6$·Py_3T was synthesized by adding **Py_3T** (0.390 mg, 1.24 μmol) to a $CDCl_3$ solution of **$Zn_3$1$(NO_2)_6$** (2.746 mg, 0.8616 μmol), stirring for a few minutes, and then filtering. This solution was made up to 0.850 mL, **Ru(CO)$Zn_2$2** was added (2.676 mg, 0.9124 μmol), and the mixture was incubated at 60 °C for 2 days. The extent of **Py_3T** transfer was calculated from the integrals of the bound **Py_3T** resonances in the 250 MHz ^1H NMR spectrum.

Acknowledgment. We thank Mr. P. Loveday and Mr. S. Wilkinson (UCL, Cambridge) for $Ru_3(CO)_{12}$, Mr. C. Sporikou (UCL, Cambridge) for benzyl 4-(2-(methoxycarbonyl)ethyl)-3,5-dimethylpyrrole-2-carboxylate, Dr. D. W. J. McCallien for **$Zn_3$1$(NO_2)_6$**, Dr. N. Bampos and Dr. D. W. J. McCallien for NMR spectra, Dr. L. Twyman for MALDI-TOF spectra, and the EPSRC Mass Spectrometry Service for FAB mass spectra. Phoenix Pharm Distributors, the Ethyl Corp., the Cambridge Commonwealth Trust, and the NZVCC provided generous financial support.

Supporting Information Available: A proton NMR spectrum of **Ru(CO)$Zn_2$2·Py_3T**, a derivation of the equation describing the binding of pyridine to **Ru(CO)3**, and a graphical representation of the data obtained from the reactions depicted in Scheme 4. This material is available free of charge via the Internet at http://pubs.acs.org.

IC000411G